Progress In Electromagnetics Research B, Vol. 8, 195–212, 2008

ELECTROMAGNETIC SCATTERING OF A FIELD KNOWN ON A CURVED INTERFACE USING CONFORMAL GAUSSIAN BEAMS

J. Hillairet and J. Sokoloff

LAME Université Paul Sabatier
113 Route de Narbonne, 31062 Toulouse Cedex, France

S. Bolioli

ONERA-DEMR
2 av. E. Belin, BP4025, 31055 Toulouse cedex, France

Abstract—Asymptotic techniques have been successfully applied to compute electromagnetic wave radiation in various high-frequency engineering domains. Recent approaches based on Gaussian beams for tracking fields may overcome some problems inherent to the ray methods such as caustics. The efficiency of these methods is based on the ability to expand surface fields into a superposition of Gaussian beams. However, some difficulties may arise when the surface is curved. In this paper, we propose a new efficient way to expand fields on a curved surface into Gaussian beams. For this purpose, a new beam formulation called Conformal Gaussian Beam (CGB) is used. The CGBs have been developed to overcome the limitation of the expansion into paraxial Gaussian Beams. The analytical Plane-Wave Spectrum and far-field of a CGB are derived and compared with numerical calculations. A brief parameter analysis of the CGBs is realised.

1. INTRODUCTION

For several years, high-frequency techniques have been successfully applied to describe electromagnetic wave radiation in various domains: antenna analysis, propagation, Radar Cross-Section computation, compatibility issues, etc. As the size of the objects under consideration tends to be large according to the wavelength, rigorous approaches such as the finite-element method (FEM) or the method of moments (MoM) become computer time and resource prohibitive. In contrast,

at sufficiently high-frequency, the electromagnetic phenomena such as radiation, propagation and diffraction, exhibit localized behavior properties [1]. As the asymptotic methods use a local description of EM fields, such as the ray techniques, their efficiency increases with the frequency.

Ray techniques like the shooting or bouncing ray methods represent the fields by a set of Geometrical Optics (GO) ray tubes for which the propagation, reflection and transmission obey the generalized Fermat's principle and the power conservation. However, some difficulties may arise with some complex situations, such as caustics. Moreover, the number of rays and the computation time may increase for complex cases such as radomes.

Current based approaches such as Physical Optics (PO) and Physical Theories of Diffraction (PTD) do not rely on the concept of ray and then can circumvent ray-based problems like caustics. However, the asymptotic evaluation of radiating fields by the PO/PTD currents needs numerical integration which can be also time and resources consuming. Many directions and techniques such as hybrid methods exist in order to deal with these theoretical and practical challenges [2, 3].

Some approaches may use different basis functions involving Gaussian Beams (GBs) for tracking fields in complex environments [4–9]. Various formulations based on Gaussian Beams are reviewed in [10]. The Gaussian Beam set ables one to reduce the number of required ray tubes and avoids caustics problems. Moreover, asymptotic methods allow to express propagation and transformation of the GBs by interfaces in closed form expressions. Gaussian Beams Tracking (GBT) methods are based on the ability to expand any source fields into a summation of Gaussian beams [11, 12]. During the last years, GBT has been successfully applied to the computation of the fields scattered by mono and multilayer dielectric radomes [13, 8]. Recently, it has been applied to the Airbus A380 front antenna radome, reducing computation time by a factor 70 in contrast with a classic Plane-Wave Spectrum (PWS) based method [14].

The source fields expansion into a superposition of GBs can be performed through different techniques. A fully rigourous method such as the Gabor frame-based expansion can be used for fields defined over a plane [11] or extended to cylindrical surfaces [15]. However, in some situations, fields are only known over a curved surface. This case occurs for example in radome engineering.

Point matching or minimum least square error can be used to express the fields on a surface as a superposition of equally spaced GBs [6]. However, this technique fails for a heavy curved surface. In

order to treat a more general class of curved surfaces, [16] proposed to use a Gabor expansion with respect to the curvilinear coordinate of a regular interface in a two-dimensional case. This expansion requires a new kind of Gaussian beams, named Conformal Gaussian Beams (CGB) [17]. The basic idea of the CGB is still to expand non-local fields into a summation of localized fields who depends on the local curvature of the surface. In this paper, we use a point matching expansion of equivalent currents on a 3D curved surface into some localized Gaussian amplitude currents. The field radiated by each of these localized currents can be expressed through a closed-form by applying standard asymptotic techniques.

In Section 2, we present the principal characteristics of the CGBs extended to the three-dimensional case. In Section 3, we derive the analytical Plane Wave Spectrum (PWS) of a CGB. A comparison with a numerical evaluation of the PWS is presented. The PWS of a CGB will able one to express the interaction between fields and dielectric interfaces as done in [13]. In Section 4 we derive the analytical far-field of a CGB. A numerical comparison with a traditional KOTTLER integration is realized for a sharp surface to demonstrate the CGB validity and to exhibit their main properties. An $\exp(+j\omega t)$ time dependence for the electromagnetic fields is assumed and suppressed throughout in this paper.

2. CONFORMAL GAUSSIAN BEAM

The expansion of a source field into a superposition of GBs can be performed on some moderate curved surface as illustrated on Fig. 1(a) In this case, the angle between the main propagation direction of the local equivalent field and the normal vector direction on the local surface is small. The local assumption is valid and the beams's half-widths (W_0) on the surface are small. On the contrary, for a heavy curved surface (Fig. 1(b)), the local assumption is not valid anymore: the beams widths may be too large leading to an incorrect expansion and to a wrong evaluation of the radiated fields.

In order to circumvent this problem, one needs to keep a finite size beam on the surface and to have the possibility to specify a main radiation direction of the beams. Conformal Gaussian Beams (CGB) combine both properties. In this section, we briefly present an extension of the CGB to the three-dimensional case. More details about CGB can be found in [13, 17].

We first assume that the electric and magnetic fields are known on a curved surface S. Equivalent electric $\mathbf{J}$ and magnetic $\mathbf{M}$ currents are then given by the Equivalence Theorem on S. As presented in [13],

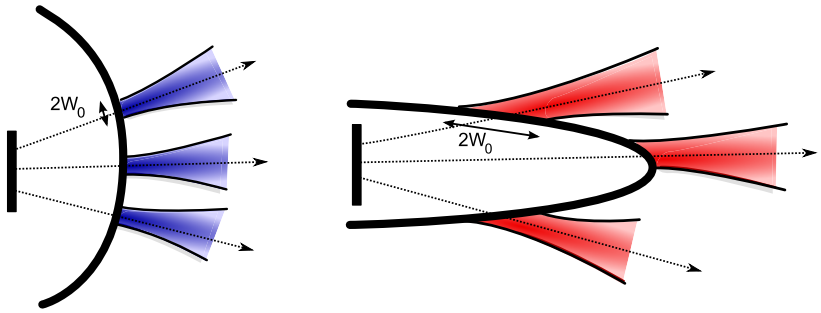

Figure 1. Illustration of the expansion of a field on a curved surface into a superposition of GBs. (a) Moderate curvature, (b) Strong curvature.

the basic idea is to expand the surface-currents $\mathbf{J}, \mathbf{M}$ using Gaussian amplitude currents:

$$\mathbf{J} = \sum_n a_n^J \hat{\mathbf{e}}_n^J(x'_n, y'_n) u(x'_n, y'_n) = \sum_n a_n^J \mathbf{J}_n^{CGB}(x'_n, y'_n) \tag{1}$$

$$\mathbf{M} = \sum_n a_n^M \hat{\mathbf{e}}_n^M(x'_n, y'_n) u(x'_n, y'_n) = \sum_n a_n^M \mathbf{M}_n^{CGB}(x'_n, y'_n) \tag{2}$$

where $\mathbf{J}_n^{CGB}$ and $\mathbf{M}_n^{CGB}$ are the electric and magnetic elementary currents. Each current is expressed in its own local coordinate system (O_n, x'_n, y'_n, z'_n) which is translated along the surface according to the order n. The $a_n^{J/M}$ terms are the expansion coefficients, $\hat{\mathbf{e}}_n^{J/M}$ the local tangent current unit-vector directions related to each elementary current and u a Gaussian function defined by:

$$\begin{aligned} u(x'_n, y'_n) = & \exp\left[-j\frac{k}{2}\begin{pmatrix} x'_n \\ y'_n \end{pmatrix}^t \mathbb{Q}_n^f \begin{pmatrix} x'_n \\ y'_n \end{pmatrix}\right] \\ & \exp\left[-j\begin{pmatrix} \beta_{x;n} \\ \beta_{y;n} \end{pmatrix} \cdot \begin{pmatrix} x'_n \\ y'_n \end{pmatrix}\right] \end{aligned} \tag{3}$$

where k is the wave number and $\mathbb{Q}_f$ the complex curvature matrix of the elementary currents, analogue to that of conventional elliptical Gaussian Beam field formulation [5].

$$\mathbb{Q}_n^f = \frac{2}{jk}\begin{pmatrix} q_{11;n}^f & q_{12;n}^f \\ q_{12;n}^f & q_{22;n}^f \end{pmatrix} \tag{4}$$

The eigenvalues of this matrix are related to the Gaussian current waists $W_{0_{x,n}}$, $W_{0_{y,n}}$ defined on the principal curvature axes by:

$$\begin{aligned}\text{eigenval}(\mathbb{Q}_n^f) \;=\; & \frac{1}{2}\left(q_{11;n}^f + q_{22;n}^f\right) \\ & \pm\frac{1}{2}\sqrt{\left(q_{11;n}^f + q_{22;n}^f\right)^2 - 4\left(q_{11;n}^f q_{22;n}^f - {q_{12;n}^f}^2\right)} \quad (5)\end{aligned}$$

$(\beta_{x;n}, \beta_{y;n})$ are the linear phase terms which define the main propagation direction of the beam fields. The fields radiated by those elementary Gaussian currents are named Conformal Gaussian Beam (CGB).

The general geometry for the problem is shown on Fig. 2. Let O be the center of the absolute frame $\{\hat{\mathbf{e}}_x, \hat{\mathbf{e}}_y, \hat{\mathbf{e}}_z\}$. As in the following we consider only one elementary CGB for the sake of clarity, subscripts n have been suppressed. The z-axis is normal to the curved surface S on O. Let $\mathbf{r} = x\hat{\mathbf{e}}_x + y\hat{\mathbf{e}}_y + z\hat{\mathbf{e}}_z$ be an observation point and $\mathbf{r}' = x'\hat{\mathbf{e}}_x + y'\hat{\mathbf{e}}_y + z'\hat{\mathbf{e}}_z$ a point on S. Unprimed characters denote the observation points and primed characters denote points on the surface S.

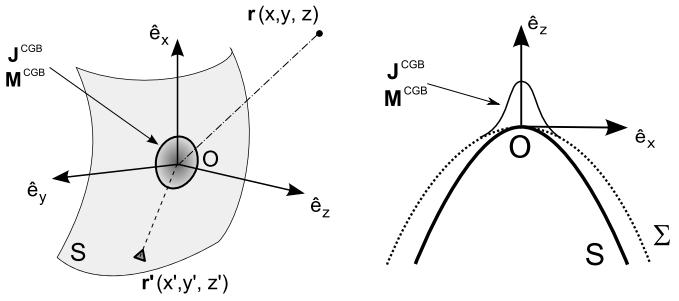

(a) (b)

Figure 2. Geometry of the problem. The surface S is approximated at O by a paraboloid Σ. An elementary current $\mathbf{J}^{CGB}$ or $\mathbf{M}^{CGB}$ is defined on O. (a) General view, (b) $(O, \hat{\mathbf{e}}_x, \hat{\mathbf{e}}_z)$ plane cut.

It is assumed that the surface S at O can be approximated locally by a paraboloid Σ. The radius of curvature of the quadric are that of the original surface at O. Therefore, z' can approximated by [5]:

$$z' \approx -\frac{1}{2}\begin{pmatrix} x' \\ y' \end{pmatrix}^t \mathbb{Q}^{\Sigma} \begin{pmatrix} x' \\ y' \end{pmatrix} \quad (6)$$

where $\mathbb{Q}^{\Sigma}$ stands for the curvature matrix which eigenvalues are the inverse of the principal local radii of curvature R_x and R_y of the surface Σ in O:

$$\mathbb{Q}^{\Sigma} = \begin{pmatrix} q_{11}^{\Sigma} & q_{12}^{\Sigma} \\ q_{12}^{\Sigma} & q_{22}^{\Sigma} \end{pmatrix} \tag{7}$$

Elementary electric and magnetic Gaussian currents $\mathbf{J^{CGB}}, \mathbf{M^{CGB}}$ are defined on Σ by:

$$\mathbf{J}^{CGB}(x', y') = \hat{\mathbf{e}}^{J}(x', y')u(x', y') \tag{8}$$

$$\mathbf{M}^{CGB}(x', y') = \hat{\mathbf{e}}^{M}(x', y')u(x', y') \tag{9}$$

Using the FRANZ's integrals [18], the radiated fields from electric $\mathbf{J}^{CGB}$ and magnetic $\mathbf{M}^{CGB}$ elementary currents can be expressed as electric $\mathbf{E}_J^r, \mathbf{H}_J^r$ and magnetic $\mathbf{E}_M^r, \mathbf{H}_M^r$ CGB by:

$$\mathbf{E}_J^r(\mathbf{r}) = \frac{Z_0}{jk}\boldsymbol{\nabla} \times \boldsymbol{\nabla} \times \mathbf{A}_J(\mathbf{r}) \tag{10a}$$

$$\mathbf{E}_M^r(\mathbf{r}) = -\boldsymbol{\nabla} \times \mathbf{A}_M(\mathbf{r}) \tag{10b}$$

$$\mathbf{H}_J^r(\mathbf{r}) = \boldsymbol{\nabla} \times \mathbf{A}_J(\mathbf{r}) \tag{11a}$$

$$\mathbf{H}_M^r(\mathbf{r}) = \frac{1}{jkZ_0}\boldsymbol{\nabla} \times \boldsymbol{\nabla} \times \mathbf{A}_M(\mathbf{r}) \tag{11b}$$

The differential operators act only on the observation point dependant terms $(\mathbf{r})$. $Z_0 = \sqrt{\frac{\mu_0}{\varepsilon_0}}$ is the free-space impedance and:

$$\mathbf{A}_M(\mathbf{r}) = \iint_{\Sigma} \mathbf{M}^{CGB}(x', y')G(\mathbf{r}, \mathbf{r}')\, dS' \tag{12}$$

$$\mathbf{A}_J(\mathbf{r}) = \iint_{\Sigma} \mathbf{J}^{CGB}(x', y')G(\mathbf{r}, \mathbf{r}')\, dS' \tag{13}$$

$$G(\mathbf{r}, \mathbf{r}') = \frac{e^{-jk\|\mathbf{r}-\mathbf{r}'\|}}{4\pi\|\mathbf{r}-\mathbf{r}'\|} \tag{14}$$

To illustrate the aspect of a CGB, we represent on Fig. 3 the numerical computation of the radiation of an elementary two-dimensional electric current $\mathbf{J}^{CGB} = \hat{\mathbf{e}}^{J}(x', y')u(x', y')$ defined at O by a KOTTLER current integral [16]. As any conventional current on a surface, elementary currents radiate toward both sides of the surface Σ. However, the radiation patterns on each side are not the same because of the curvature of the surface.

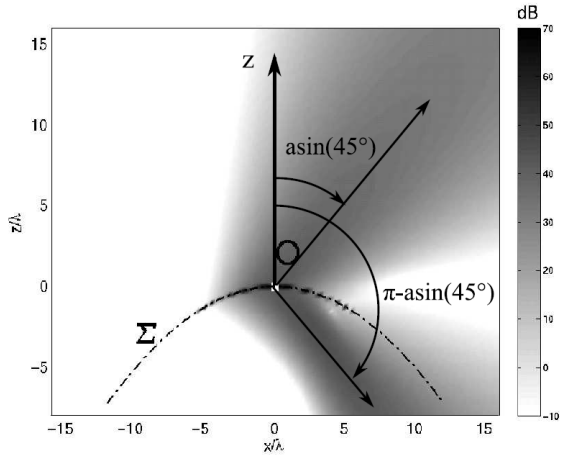

Figure 3. Example of electric field radiated by a single two-dimensional elementary electric current $\mathbf{J}^{CGB}$ defined at 0 with $W_{0_x} = 2\lambda$, $R_x = 10\lambda$ and $\beta_x = k\sin(45°)$. The elementary current radiates in two main directions which are given by the value of the β_x parameter.

On the contrary of a classical Gaussian beam for which the source is located at infinity, the source of a CGB is localized on the surface. Moreover, a CGB has two main propagation directions and depends on the local properties of the surface.

3. CGB PLANE-WAVE SPECTRUM

3.1. Plane-wave Spectrum Derivation

In this section, we derive the asymptotic expression of the Plane-Wave Spectrums (PWS) $\tilde{\mathbf{E}}, \tilde{\mathbf{H}}$ of a CGB, which are defined by:

$$\mathbf{E}^r(\mathbf{r}) = \frac{1}{4\pi^2} \iint_{-\infty}^{+\infty} \tilde{\mathbf{E}}(k_x, k_y) e^{-j(k_x x + k_y y + k_z z)} dk_x\, dk_y \qquad (15)$$

$$\mathbf{H}^r(\mathbf{r}) = \frac{1}{4\pi^2} \iint_{-\infty}^{+\infty} \tilde{\mathbf{H}}(k_x, k_y) e^{-j(k_x x + k_y y + k_z z)} dk_x\, dk_y \qquad (16)$$

In order to express these spectrum, the spatial integrals (12) and (13) issued from Franz formulations can be transformed into spatial and spectral integrals by expanding the free-space Green function $G(\mathbf{r}, \mathbf{r}')$ into its Plane-Wave Spectrum using the Weyl

expansion [19, p.481]:

$$G(\mathbf{r},\mathbf{r}') = \frac{1}{8j\pi^2}\iint_{-\infty}^{+\infty} e^{-j(k_x(x-x')+k_y(y-y')+k_z|z-z'|)}\,\frac{dk_x\,dk_y}{k_z} \tag{17}$$

where

$$k_z = \begin{cases} \sqrt{k^2-k_x^2-k_y^2}, & \text{if } k^2 > k_x^2+k_y^2 \\ -j\sqrt{k_x^2+k_y^2-k^2}, & \text{if } k^2 < k_x^2+k_y^2 \end{cases} \tag{18}$$

For complex values of k_x and k_y, the convergence of the integral is guaranteed by imposing the square root condition $\mathrm{Im}[k_z] < 0$. Pole singularities may be avoided by introducing small losses ($\mathrm{Im}[k] = 0^-$), which are eventually removed [19]. Later on, we assume that $z > z'$, and we remove the modulus sign on $z - z'$ in (17). The procedure is the same in far zone for $z < z'$. Substituting (17) into the integral expression (12) and (13) and interchanging the order of spatial and spectral integration [20, 21], one can evaluate the spatial integral by the method of the saddle point and then express the fields as a spectral integral. Details of the calculus can be found on the Appendix A. Finally, we deduce by identification from the Equations (15) and (16) the analytical Plane-Wave Spectrums of a Conformal Gaussian Beam:

$$\tilde{\mathbf{E}}(k_x,k_y) = \left[\frac{Z_0}{k}\left(\mathbf{k}\times\mathbf{k}\times\hat{\mathbf{e}}^J\right) + \left(\mathbf{k}\times\hat{\mathbf{e}}^M\right)\right]\frac{\gamma(k_x,k_y)}{2k_z} \tag{19}$$

$$\tilde{\mathbf{H}}(k_x,k_y) = \left[\left(-\mathbf{k}\times\hat{\mathbf{e}}^J\right) + \frac{1}{Z_0 k}\left(\mathbf{k}\times\mathbf{k}\times\hat{\mathbf{e}}^M\right)\right]\frac{\gamma(k_x,k_y)}{2k_z} \tag{20}$$

where the expression of $\gamma(k_x,k_y)$ is given in appendix. One can note that the derivation does not depend on a paraxial approximation. Therefore, the analytical Plane-Wave Spectrum of a CGB can be used beyond the paraxial limitation which relates to some conventional GBs formulations.

3.2. Numerical Results

In order to validate preceding results, a comparison between the analytical and a numerical computation of the PWS has been performed. First, the fields radiated by an elementary electric current $\mathbf{J}^{CGB}$ are evaluated on a plane surface Λ near the radiating surface Σ by a numerical current integration. Then, the PWS of the field on this plane surface is computed and compared with our analytical formulation (19). The geometry of the test case is depicted on Fig. 4. Results are presented on Fig. 5 and Fig. 6.

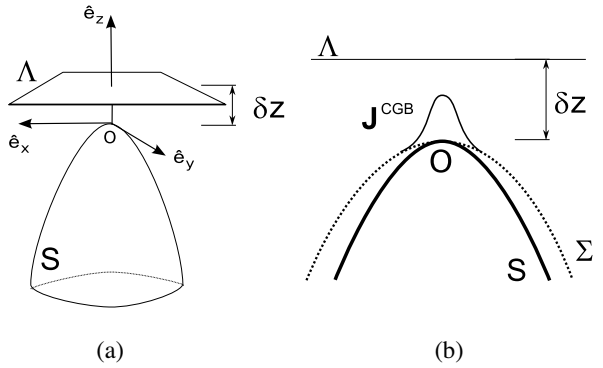

Figure 4. Geometry for the numerical validation of the PWS of a CGB. The plane surface Λ is upper the curved surface S where an elementary electric current $\mathbf{J}^{CGB}$ is defined in O. The radiated field on Λ is computed by a numerical Kottler radiation integration. Then, the PWS of the fields is computed on the plane Λ and compared to the analytical expression (19). (a) General view, (b) $\hat{\mathbf{e}}_x$, $\hat{\mathbf{e}}_z$ plane cut.

4. CGB FAR-FIELD

4.1. Far-Field Derivation

We derive here the asymptotic approximation for large value of kr of a CGB ($r = \|\mathbf{r}\|$) for the half-plane $z > 0$. For the sake of brevity, the development is only performed for the $\mathbf{E}^r$ field. The same results can be obtained for the magnetic field. We rewrite Equation (15) into the following general compact form

$$\mathbf{E}^r(\mathbf{r}) = \frac{1}{4\pi^2} \iint_{-\infty}^{+\infty} \tilde{\mathbf{E}}(k_x, k_y) e^{jkr\Psi(\mathbf{k})}\, dk_x\, dk_y \tag{21}$$

with

$$\Psi(\mathbf{k}) = -\frac{1}{kr}\mathbf{k}\cdot\mathbf{r} = -\frac{1}{kr}(k_x x + k_y y + k_z z) \tag{22}$$

The approximation may be obtained by the application of stationary phase method for double integrals [19], and one obtains:

$$\mathbf{E}^r(r,\theta,\phi) \approx \frac{jk}{2\pi}\cos\theta \frac{e^{-jkr}}{r} \tilde{\mathbf{E}}(k\sin\theta\cos\phi, k\sin\theta\sin\phi) \quad -\frac{\pi}{2} < \theta < \frac{\pi}{2}, \forall\phi \in [0,\pi] \tag{23}$$

where (r,θ,ϕ) are the spherical coordinates with origin O.

4.2. Numerical Results

The far-field expression (23) is compared to a numerical computation based on the Kottler integrals for the electric field radiated by an elementary current $\mathbf{J}^{CGB} = \hat{\mathbf{e}}^J(x', y')u(x', y')$. The unit vector $\hat{\mathbf{e}}^J(x', y')$ is defined as $\hat{\mathbf{e}}^J(0, 0) = \hat{\mathbf{e}}_y$. $\mathbf{J}^{CGB}$ is defined on the local

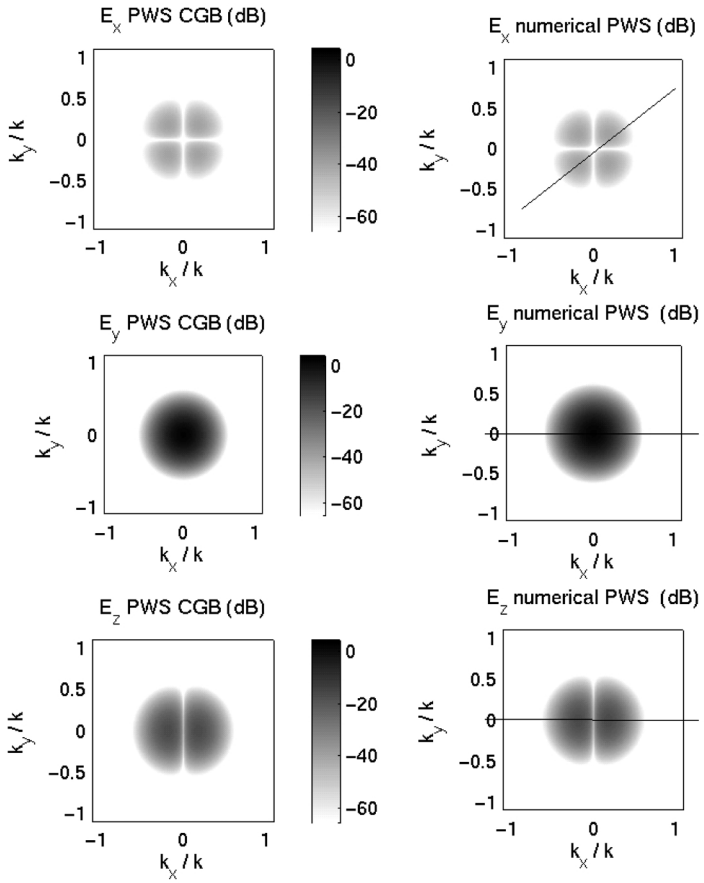

Figure 5. Comparisons between analytical Plane Wave Spectrum (PWS) of a Conformal Gaussian Beam with a numerical PWS computation of the field calculated on the plane Λ. We represent here the three components $\tilde{\mathbf{E}}_x, \tilde{\mathbf{E}}_y, \tilde{\mathbf{E}}_z$ of the PWS. Plain lines symbolize the cuts represented on Fig. 6. $\mathbf{J}^{CGB} = \hat{\mathbf{e}}^J(x', y')u(x', y')$, $\mathbf{M}^{CGB} = \mathbf{0}$, $W_0 = 2\lambda$, $R_x = R_y = 10\lambda$, $\delta z = 1\lambda$, $\beta_x = \beta_y = 0$. Unit-vector $\hat{\mathbf{e}}^J$ is defined as $\hat{\mathbf{e}}^J(0, 0) = \hat{\mathbf{e}}_y$.

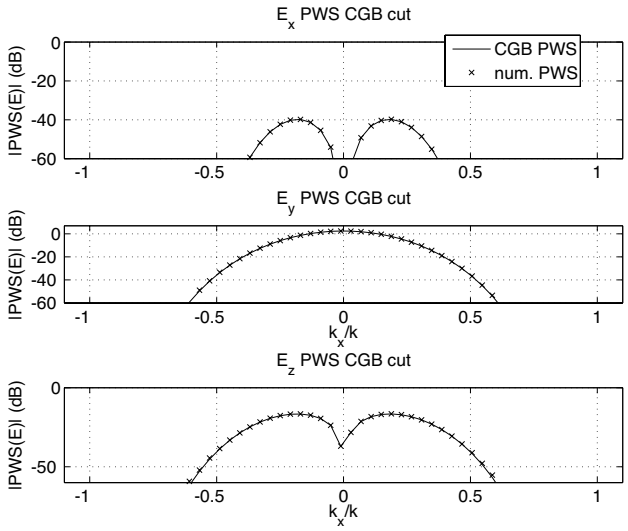

Figure 6. Profiles of the three components of the PWS of a CGB. $\mathbf{J}^{CGB} = \hat{\mathbf{e}}^J(x', y')u(x', y')$, $\mathbf{M}^{CGB} = \mathbf{0}$, $W_0 = 2\lambda$, $R_x = R_y = 10\lambda$, $\delta z = 1\lambda$, $\beta_x = \beta_y = 0$.

system (O, x, y, z), as represented on Fig. 2. The fields are evaluated at large distance R. Results are shown on Fig. 7. Due to the fact that we used only one electric current for the sake of simplicity, one can note there are two beams radiated above and below the surface, as on the Fig. 3. However, in applications involving dielectric interfaces, currents on the surface are both electric and magnetic in vertu of the Equivalence theorem. Then, because of mutual destructive interference between fields radiated by both type of currents, there is only one beam radiated. In the next paragraphs, a brief parameter study of a CGB is realised, in order to show its principal properties. For each of these cases, numerical comparisons with a numerical Kottler current radiation integral show the same accuracy as seen on Fig. 7.

We define the CGB circular: $W_{0_x} = W_{0_y} = W_0$. One elementary electric current $\mathbf{J}^{CGB}$ is considered for all the examples, defined on O and oriented on the $\hat{\mathbf{e}}^J(0, 0) = \hat{\mathbf{e}}_y$ axis. When the surface is a perfect plane ($R_x = R_y = \infty$), the beam size tends to decrease as the waist size increases. This result confirms that on a plane surface, elementary currents radiate like the currents which would be induced by a conventional Gaussian beam. One effect of the surface curvature is visible on Fig. 8 where the principal radii of curvature are $R_x = R_y = 10\lambda$ and W_0 varies from 1λ to 10λ. CGB are not anymore

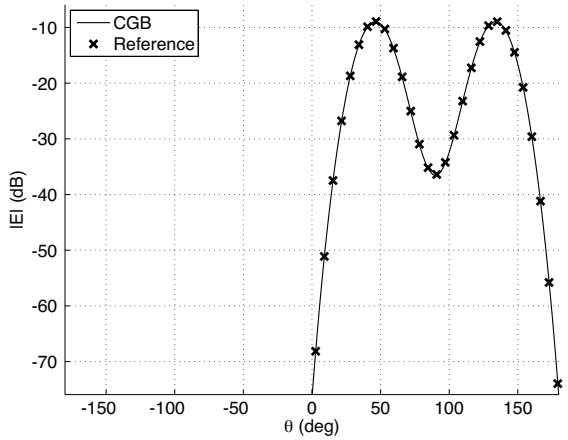

Figure 7. Electric far-field of a CGB compared to a Kottler numerical radiation integral (Reference). The geometry of the problem is depicted on Fig. 2. $\mathbf{J}^{CGB} = \hat{\mathbf{e}}^J(x', y')u(x', y')$, $W_0 = 2\lambda$, $R_x = R_y = 10\lambda$ and $\beta_x = k\sin(45°)$, $\beta_y = 0$.

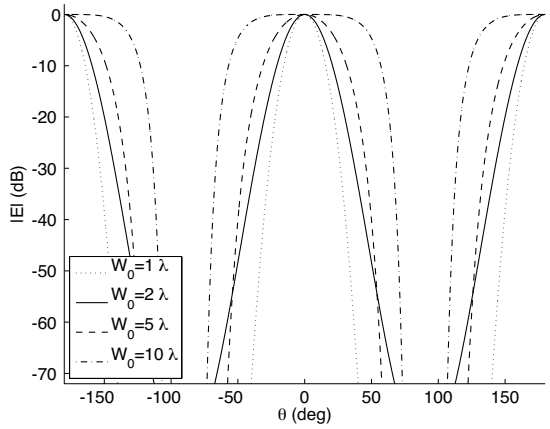

Figure 8. Normalized electric far-fields comparison of a CGB for different values of W_0 on a curved surface ($R_x = R_y = 10\lambda$) for $W_0 = 1, 2, 5$ and 10λ. $\beta_x = \beta_y = 0$.

close to conventional GB, because the size of the beam raises when the waist increases.

On Fig. 9, we have represented some normalized E-field for different values of the principal radii of curvature $R_x = R_y = \infty$, $30, 10$ and 5λ while W_0 is set to 2λ. As the curvature of the surface

increases, the size of the beam increases also.

On Fig. 10, we have represented some normalized E-field for different values of the linear phase term β_x corresponding to a main propagation direction angle varying from 0° to 85° ($\beta_y = 0$). The

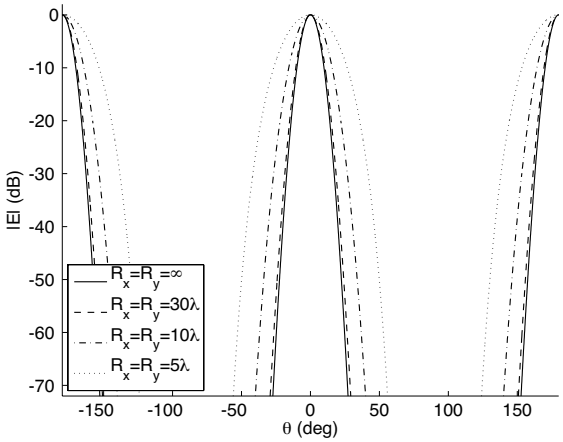

Figure 9. Normalized electric far-fields comparison of a CGB for different values of the principal radii of curvature (R_x, R_y) of the surface for $R_x = R_y = \infty$ (perfect plane), $30, 10$ and 5λ with $W_0 = 2\lambda$. $\beta_x = \beta_y = 0$.

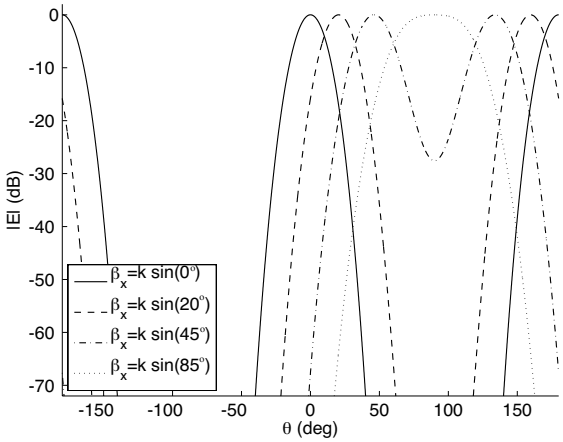

Figure 10. Normalized electric far-fields comparison of a CGB for different values of the linear phase term (β_x, β_y) for $\beta_x = k\sin(0°), k\sin(20°), k\sin(45°)$ and $k\sin(85°)$, $\beta_y = 0$. $R_x = R_y = 10\lambda$ and $W_0 = 2\lambda$.

curvature radii are set to 10λ and W_0 to 2λ. One notes that both radiated beams tends to form a unique beam as the angle from the $\hat{\mathbf{e}}_z$ axis increases.

5. CONCLUSION

The Conformal Gaussian Beams (CGB) have been presented. These new beams are radiated by elementary Gaussian currents on a curved surface. Using the FRANZ field integral and the WEYL expansion of the free-space Green function, a closed form of the plane-wave spectrum (PWS) of a CGB has been obtained. A comparison between a numerical evaluation of the PWS and the analytical form has been made. The far-field of a CGB has been expressed and compared with a classical numerical current integration method. A very good agreement is observed. A brief parameter study has been realised in order to exhibit the main properties of the CGB.

A multi-beams summation can been applied in three-dimensional problems to expand electric and magnetic currents on a curved interface into elementary Gaussian currents as done in the two-dimensional case [17]. With the analytical plane-wave spectrum of a CGB and using the Fresnel coefficients, a closed-form calculation of the reflected and transmitted fields by a mono or multi dielectric layers curved interface is possible as realised in [13]. These will be presented in future communications.

APPENDIX A. DERIVATION OF THE PWS OF A CGB

Substituting Equation (17) into Equations (12) and (13) and interchanging the order of spatial and spectral integration, one obtains:

$$\mathbf{A}_M(\mathbf{r}) = \frac{1}{8j\pi^2} \iint_{-\infty}^{+\infty} \frac{\overline{\mathbf{U}}_M(k_x, k_y)}{k_z} e^{-j(k_x x + k_y y + k_z z)}\, dk_x\, dk_y$$

$$\mathbf{A}_J(\mathbf{r}) = \frac{1}{8j\pi^2} \iint_{-\infty}^{+\infty} \frac{\overline{\mathbf{U}}_J(k_x, k_y)}{k_z} e^{-j(k_x x + k_x y + k_z z)}\, dk_x\, dk_y$$

with

$$\overline{\mathbf{U}}_M(k_x, k_y) = \iint_{\Sigma} \mathbf{M}^{CGB}(x', y') e^{+j(k_x x' + k_y y' + k_z z')}\, dS' \qquad \text{(A1)}$$

$$\overline{\mathbf{U}}_J(k_x, k_y) = \iint_{\Sigma} \mathbf{J}^{CGB}(x', y') e^{+j(k_x x' + k_y y' + k_z z')}\, dS' \qquad \text{(A2)}$$

We now evaluate the last two integrals. By substituting $\mathbf{J}^{CGB}$ and $\mathbf{M}^{CGB}$ by their expressions (8) and (9), one obtains:

$$\overline{\mathbf{U}}_M(k_x,k_y) = \iint_\Sigma \hat{\mathbf{e}}^M(x',y')u(x',y')e^{+j(k_xx'+k_yy'+k_zz')}\,dS' \tag{A3}$$

$$\overline{\mathbf{U}}_J(k_x,k_y) = \iint_\Sigma \hat{\mathbf{e}}^J(x',y')u(x',y')e^{+j(k_xx'+k_yy'+k_zz')}\,dS' \tag{A4}$$

where the surface element dS' for the quadric surface Σ (6) is given for cartesian coordinates by,

$$dS' = \sqrt{1+\left(\frac{\partial z'}{\partial x'}\right)^2+\left(\frac{\partial z'}{\partial y'}\right)^2}\,dx'dy' = \sqrt{d(x',y')}dx'dy' \tag{A5}$$

Using (3) and (6), we put those integrals under a general reduced form:

$$\overline{\mathbf{U}}_i(k_x,k_y) = \iint_{-\infty}^{+\infty} \boldsymbol{\psi}^i(x',y')e^{-k\Phi(x',y')}\,dx'\,dy' \tag{A6}$$

where the subscript i denotes either M or J, and

$$\boldsymbol{\psi}^i(x',y') = \hat{\mathbf{e}}^i(x',y')\sqrt{d(x',y')} \tag{A7}$$

$$\Phi(x',y') = \frac{j}{2}\begin{pmatrix}x'\\y'\end{pmatrix}^t\mathbb{Q}\begin{pmatrix}x'\\y'\end{pmatrix} - \frac{j}{k}\begin{pmatrix}x'\\y'\end{pmatrix}^t\cdot\begin{pmatrix}k_x-\beta_x\\k_y-\beta_y\end{pmatrix} \tag{A8}$$

$q_{mn} = q^f_{mn} + \frac{k_z}{k}q^\Sigma_{mn}$ represents the elements of the matrix $\mathbb{Q}$. Integral (A6) has an appropriate form to be evaluated with the saddle-point method for complex double integral [22]:

$$\overline{\mathbf{U}}_i(k_x,k_y) \simeq \hat{\mathbf{e}}^i(x'_s,y'_s)\gamma(k_x,k_y) \tag{A9}$$

where (x'_s,y'_s) are the coordinates of the saddle point given by

$$\begin{pmatrix}x'_s\\y'_s\end{pmatrix} = \frac{\mathbb{Q}^{-1}}{k}\begin{pmatrix}k_x-\beta_x\\k_y-\beta_y\end{pmatrix} \tag{A10}$$

and

$$\gamma(k_x,k_y) = \frac{2\pi}{k}\sqrt{d(x'_s,y'_s)}\,(-\det\mathbb{Q})^{-\frac{1}{2}} \exp\left[\frac{j}{2k}\begin{pmatrix}k_x-\beta_x\\k_y-\beta_y\end{pmatrix}^t\mathbb{Q}^{-1}\begin{pmatrix}k_x-\beta_x\\k_y-\beta_y\end{pmatrix}\right] \tag{A11}$$

In Equations (10) and (11), the curl operators can operate inside the spectral integral because the derivative operates only on the observation point ($\mathbf{r}$) dependant parameters, merely the $\exp(-j\mathbf{k}\cdot\mathbf{r})$ term. One obtains,

$$\mathbf{E}_J^r(\mathbf{r}) = \frac{1}{4\pi^2}\iint_{-\infty}^{+\infty} \frac{Z_0}{k}\left(\mathbf{k}\times\mathbf{k}\times\hat{\mathbf{e}}^J\right)\frac{\gamma(k_x,k_y)}{2k_z}e^{-j\mathbf{k}\cdot\mathbf{r}}dk_x\,dk_y \quad \text{(A12a)}$$

$$\mathbf{E}_M^r(\mathbf{r}) = \frac{1}{4\pi^2}\iint_{-\infty}^{+\infty} \left(\mathbf{k}\times\hat{\mathbf{e}}^M\right)\frac{\gamma(k_x,k_y)}{2k_z}e^{-j\mathbf{k}\cdot\mathbf{r}}dk_x\,dk_y \quad \text{(A12b)}$$

$$\mathbf{H}_J^r(\mathbf{r}) = \frac{1}{4\pi^2}\iint_{-\infty}^{+\infty} \left(-\mathbf{k}\times\hat{\mathbf{e}}^J\right)\frac{\gamma(k_x,k_y)}{2k_z}e^{-j\mathbf{k}\cdot\mathbf{r}}dk_x\,dk_y \quad \text{(A13a)}$$

$$\mathbf{H}_M^r(\mathbf{r}) = \frac{1}{4\pi^2}\iint_{-\infty}^{+\infty} \frac{1}{Z_0 k}\left(\mathbf{k}\times\mathbf{k}\times\hat{\mathbf{e}}^M\right)\frac{\gamma(k_x,k_y)}{2k_z}e^{-j\mathbf{k}\cdot\mathbf{r}}dk_x\,dk_y \quad \text{(A13b)}$$

One recognizes in Equations (A12) and (A13) the Plane-Wave Spectrums of the radiated fields $\mathbf{E}^r$ and $\mathbf{H}^r$ as defined by Equations (15) and (16).

REFERENCES

1. Pathak, P. H., "High-frequency techniques for antenna analysis," *Proc. of the IEEE*, Vol. 80, No. 1, 44–65, Jan. 1992.
2. Felsen, L. B. and L. Sevgi, "Electromagnetic engineering in the 21st century: Challenges and perspectives," *Turk J. Elec. Engin.*, Vol. 10, No. 2, 131–145, 2002.
3. Bouche, D. P., F. A. Molinet, and R. Mittra, "Asymptotic and hybrid techniques for electromagnetic scattering," *Proc. of the IEEE*, Vol. 81, No. 12, 1658–1684, Dec. 1993.
4. Felsen, L. B., "Real spectra, complex spectra, compact spectra," *J. Opt. Soc. Am. A*, Vol. 3, No. 4, 486–496, Apr. 1986.
5. Chou, H.-T. and P. H. Pathak, "Uniform asymptotic solution for electromagnetic reflexion and diffraction of an arbitrary Gaussian beam by a smooth surface with an edge," *Radio Science*, Vol. 32, No. 4, 1319–1336, 1997.
6. Chou, H.-T. and P. H. Pathak, "Use of Gaussian ray basis functions in ray tracing methods for applications to high frequency wave propagation problems," *IEE Proceedings — Microwaves, Antennas and Propagation*, Vol. 147, No. 2, 77–81, Apr. 2000.
7. Chou, H.-T., P. H. Pathak, and R. J. Burkholder, "Novel Gaussian beam method for the rapid analysis of large reflector antennas,"

IEEE Trans. Antenna Propagat., Vol. 49, No. 6, 880–893, June 2001.

8. Lugara, D., A. Boag, and C. Letrou, "Gaussian beam tracking through a curved interface: Comparison with a method of moments," *IEE Proceedings — Microwaves, Antennas and Propagation*, Vol. 150, No. 1, 49–55, Feb. 2003.
9. Tahri, R., D. Fournier, S. Collonge, G. Zaharia, and G. El Zein, "Efficient and fast Gaussian beam-tracking approach for indoor-propagation modeling," *Microwave and Optical Technology Letters*, Vol. 45, No. 5, 378–381, 2005.
10. Heyman, E. and L. B. Felsen, "Gaussian beam and pulsed-beam dynamics: Complex-source and complex-spectrum formulations within and beyond paraxial asymptotics," *J. Opt. Soc. Am. A*, Vol. 18, No. 7, 1588–1610, July 2001.
11. Lugara, D. and C. Letrou, "Alternative to Gabor's representation of plane aperture radiation," *Electronics Letters*, Vol. 34, No. 24, 2286–2287, Nov. 1998.
12. Sokoloff, J., S. Bolioli, and P.-F. Combes, "Gaussian beam expansion for radiation analysis of metallic reflectors illuminated under oblique incidence," *IEEE Trans. on Magnetics*, Vol. 38, No. 2, 697–700, Mar. 2002.
13. Chabory, A., J. Sokoloff, S. Bolioli, and P.-F. Combes, "Computation of electromagnetic scattering by multilayer dielectric objects using Gaussian beam based techniques," *C. R. Physique*, Vol. 6, 654–662, 2005.
14. Bolioli, S., J. Sokoloff, and A. Chabory, "Multilayer radome computation — Comparison between Gaussian beam formalism and plane wave spectrum — Application to airbus a380," *ICEAA, Turino (Italy)*, Sept. 2005.
15. Letrou, C., A. Boag, and E. Heyman, "Gaussian beams representation based on periodic frames for radiation from cylindrical apertures," *IEEE/AP-S and URSI Meeting, Monterey (CA), USA*, 1979–1982, June 2004.
16. Chabory, A., S. Bolioli, and J. Sokoloff, "Novel Gabor-based Gaussian beam expansion for curved aperture radiation in dimension two," *Progress In Electromagnetics Research*, PIER 58, 171–185, 2006.
17. Chabory, A., J. Sokoloff, and S. Bolioli, "Physically based expansion on conformal Gaussian beams for the radiation of curved aperture in dimension 2," *Microwaves, Antennas and Propagation, IET*, Vol. 2, No. 2, 152–157, 2008.

18. Tai, C.-T., "Direct integration of field equations," *Progress In Electromagnetics Research*, PIER 28, 339–359, 2000.
19. Felsen, L. B. and N. Marcuvitz, *Radiation and Scattering of Waves*, IEEE Press, New York, 1994.
20. Nagamune, A. and P. H. Pathak, "An efficient plane wave spectral analysis to predict the focal region fields of parabolic reflector antennas for small and wide angle scanning," *IEEE Trans. Antenna Propagat.*, Vol. 38, No. 11, 1746–1756, Nov. 1990.
21. Ansbro, A. P. and J. M. Arnold, "Spectral asymptotics for general curved reflecting surface," *J. Opt. Soc. Am. A*, Vol. 10, No. 4, 590–599, Apr. 1993.
22. Delabaere, E. and C. Howls, "Global asymptotics for multiple integrals with boundaries," *Duke Math. J.*, Vol. 112, No. 2, 199–264, 2002.